JOURNAL OF APPLIED ELECTROCHEMISTRY **28** (1998) 71–79

Electrodeposition of Co–Ni alloys

E. GÓMEZ, J. RAMIREZ, E. VALLÉS

Departament de Química-física, Laboratori de Ciència i Tecnologia Electroquímica dels Materials, Universitat de Barcelona, Martí i Franquès, 1, 08028 Barcelona, Spain

Received 14 October 1996; revised 24 June 1997

Cobalt–nickel alloys were electrodeposited in an acid bath containing various ratios of metallic cations. The effect of the plating variables on the composition and morphology of the deposits obtained on vitreous carbon electrodes was investigated. Different proportions of the two metals can be obtained by using different deposition parameters, but at all Co(II)/Ni(II) ratios studied, preferential deposition of cobalt occurs and anomalous codeposition takes place. For a fixed solution composition, the nickel content in the deposit is enhanced by increasing the deposition potential. More homogeneous and fine-grained deposits can be obtained by increasing the cobalt(II)/nickel(II) ratio in solution and by ensuring that deposition takes place slowly. Deposits of constant composition throughout the depth of the deposit can be obtained only by stirring the solution during the deposition. In addition, the solution must be stirred in order to minimize the increase in local pH and to prevent hydroxide precipitation. An attempt was made to explain the anomalous codeposition. The results suggest the following sequence of events: first, nickel is deposited; then, cobalt(II) adsorbs onto the freshly deposited nickel and begins to be deposited. The cobalt(II) adsorption inhibits subsequent deposition of nickel, although it does not block it completely.

1. Introduction

Amorphous ferromagnetic films are widely used in the microelectronics industry, magnetic media and computer science [1]. Different methods can be used in the preparation of these films [2]. Electrodeposition is one possible way of preparing these films and, given the simplicity of the apparatus required to grow the deposits, has obvious advantages over the processes that use a vacuum system such as sputtering.

Interest in the electroplating of different alloys, like nickel–iron, developed mainly due to the magnetic properties of these films. Specifically, permalloy (nickel–iron alloy with 20% of iron by weight) has been used in several magnetic device applications [3–5]. However, other alloys such as cobalt–nickel may be appropriate. As cobalt–nickel forms a solid solution over the whole concentration range [6], the ability of nickel and cobalt to alloy in all proportions enables the potential uses of their magnetic properties to be explored in a wider range of conditions. This made cobalt–nickel alloy of especial interest to the microelectronics industry. Moreover, these Co–Ni films are expected to show a greater resistance to corrosion than Ni–Fe films.

The electrodeposition of Co–Ni, whether from simple or complex baths, occurs in an anomalous type in which the less noble metal is preferentially reduced [7–9]. In general it is important to control the electrodeposition parameters to obtain suitable deposits. In particular, for the preparation of magnetic Co–Ni alloys, the conditions to minimize the coevolution of hydrogen. For this, chloride media and intermediate solution pH were chosen for this study.

The first objective of this study was to evaluate the influence of the deposition parameters on both the composition and the morphology of the final thin electrodeposited films and to minimize h.e.r. (hydrogen evolution reaction), as far as possible in each case, to obtain deposits with the desired performance.

An attempt to establish the cause of the anomalous codeposition for the formation of Co–Ni alloys constitutes the second objective of this work, that is, to determine the reason why cobalt deposits preferentially although it is the minority species in solution.

As a first step towards our objectives, both vitreous carbon substrate and low total metallic cation concentration were selected to allow the basic deposition process.

2. Experimental details

The electrochemical experiments were carried out in a conventional three-electrode cell. Potentiostatic and potentiodynamic experiments were performed using both an EG&G model 363 potentiostat–galvanostat with IR compensation together with a PAR 175 signal generator and a Philips 8133 X–Y recorder, and an EG&G model 273 potentiostat/galvanostat controlled by a microcomputer. The latter instrument was also used for the galvanostatic experiments. The morphology of deposits was examined with a Leica Cambridge Stereoscan S-360 scanning electron microscope. The electrodeposits were analysed using the X-ray analyser incorporated in a Cambridge L-120 scanning electron microscope.

0021-891X

The electrolyte solutions were freshly prepared from $NiCl_2.6H_2O$, $CoCl_2.6H_2O$ and NaCl; the total chloride concentration was maintained at 1 mol dm^{-3}. The solution pH was adjusted to 3 with HCl in all experiments. The deposition was performed at pH 3 and from chloride solutions in order to decrease deposition potential and to prevent hydrogen evolution. All reagents were analytical grade from Merck; water was distilled twice and then treated with a Millipore Milli Q system. Before each experiment, solutions were deaerated with argon.

Vitreous carbon was used for both working and counter electrodes. The working electrode was a rotating disc electrode (RDE) of 0.07 cm^2. The rotation was selected at 1000 rpm in order to emulate the value of normal industrial stirring. The vitreous carbon electrode was polished to a mirror finish before each run, using alumina of different grades (3.75, 1.87 and 0.3 μm), and cleaned ultrasonically for 2 min in water. The reference electrode was a Ag/AgCl mounted in a Luggin capillary containing 1 mol dm^{-3} NaCl solution. All potentials were referred to this electrode. All electrodes were from Metrohm.

Stripping analysis (ALSV-anodic linear sweep voltammetry) were performed immediately after potentiostatic deposition without removing the electrode from the solution; in each case an initial potential for which deposition does not occur was selected.

3. Results

3.1. *Voltammetric experiments*

First, the voltammetric technique was used to gain information about the general behaviour of the deposition process.

A study of the deposition of both nickel from a nickel solution and cobalt from a cobalt solution was performed in order to identify the reference behaviour that would later permit the reciprocal influence in solution to be established. The concentration was fixed at 0.1 mol dm^{-3} and, in order to compare the response, the voltammograms were recorded in the same conditions, including cathodic limit.

Figure 1 shows the voltammograms when the scan was reversed at −1100 mV. For both metals, negative

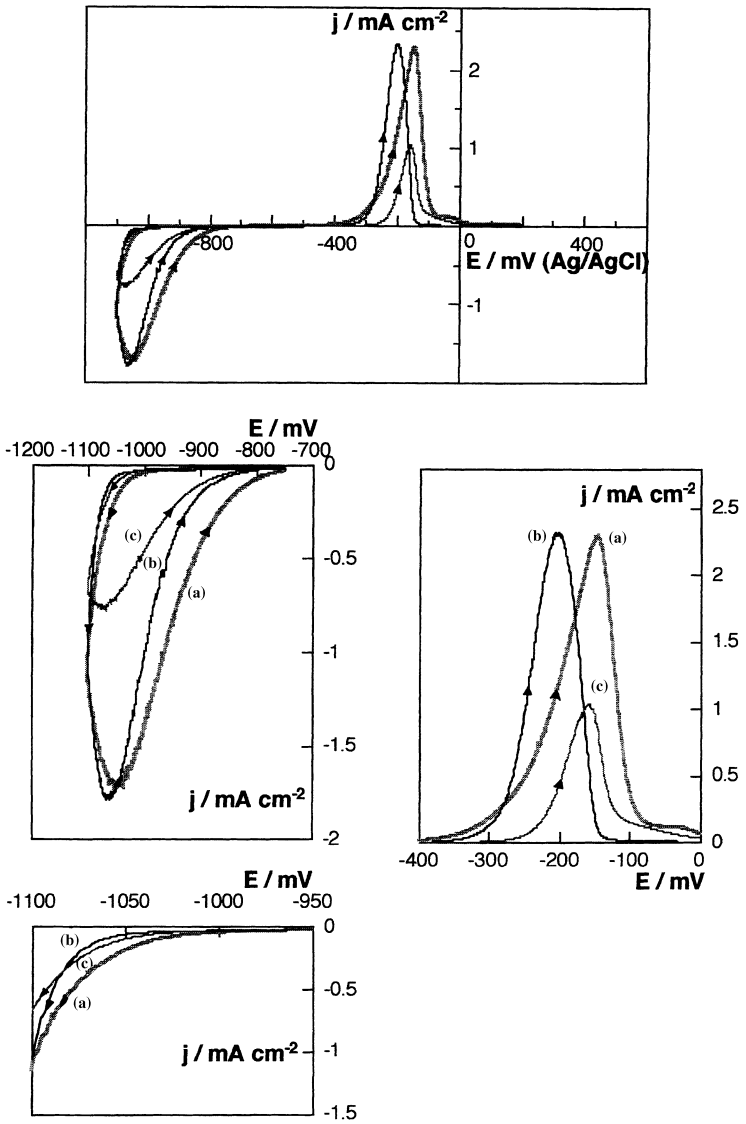

Fig. 1. Cyclic voltammograms at fixed cathodic limit: −1100 mV, $v = 50$ mV s^{-1}. General voltammograms and magnified details: (a) 0.1 mol dm^{-3} $NiCl_2$, (b) 0.1 mol dm^{-3} $CoCl_2$ and (c) 0.1 mol dm^{-3} $NiCl_2$ + 0.007 mol dm^{-3} $CoCl_2$.

current was observed in the positive going sweep, as corresponded to a nucleation process, and an oxidation peak was obtained that included the entire oxidation charge for these limits. For both metals, the appearance of the voltammetric reduction current took place at close potentials (Fig. 1, curves (a) and (b)). However, when the beginning of the deposition processes is shown at greater magnification, it is always observed that faradaic current corresponding to nickel deposition is obtained from more positive potentials than that corresponding to the cobalt.

Moreover, for cobalt deposition, the rising part of voltammetric cathodic current has a greater slope than that corresponding to nickel deposition, that is, cobalt deposition is faster. At this low limit, although the deposition of cobalt began later, the charge recorded for both metals was similar. Upon increasing the cathodic potential limit the charge recorded for cobalt was always greater than that corresponding to nickel. At this cathodic limit (-1100 mV), the peak corresponding to the oxidation of cobalt appeared at around -200 mV, 60 mV before that corresponding to the oxidation peak of nickel (Fig. 1, curves (a) and (b)).

However, the potential of the maximum of these peaks could not be taken as a reference because the voltammetric cathodic limit greatly influenced the exact position of the maximum of the oxidation peak, especially for the nickel, which constituted a great disadvantage due to the proximity of two peaks.

Since the start of the deposition process of these two metals took place at very similar potentials when they were deposited separately, special interest was placed on achieving good reproducibility of the experimental results to ensure the electrochemical response.

Initially, to study the process of Co–Ni deposition, as this alloy corresponds to an anomalous codeposition, different additions of Co(II) to 0.1 mol dm^{-3} $NiCl_2$ solution were made, but Ni(II) was always maintained as the predominant species. For each set of experiments the voltammetric response was always analysed at fixed cathodic potential limit.

Surprisingly, with a low addition of Co(II) the total charge recorded diminished drastically (Fig. 1, curve (c)), although no significant changes in the voltammogram were observed. A typical nucleation loop appeared when the scan was reversed to anodic potentials, indicating that nucleation and a three-dimensional growth process dominated the alloy deposition process and a single oxidation peak was observed. When the zone of the beginning of the voltammetric current was magnified, both a delay in the appearance of current and a marked decrease in the slope of the j/E curve were observed (Fig. 1).

Taking this result into account, a systematic study of Co(II) additions was performed. When the Co(II) concentration was very low (Fig. 2, curve (a)) a clear inhibition of nickel deposition was observed. With subsequent Co(II) additions, the process was slightly

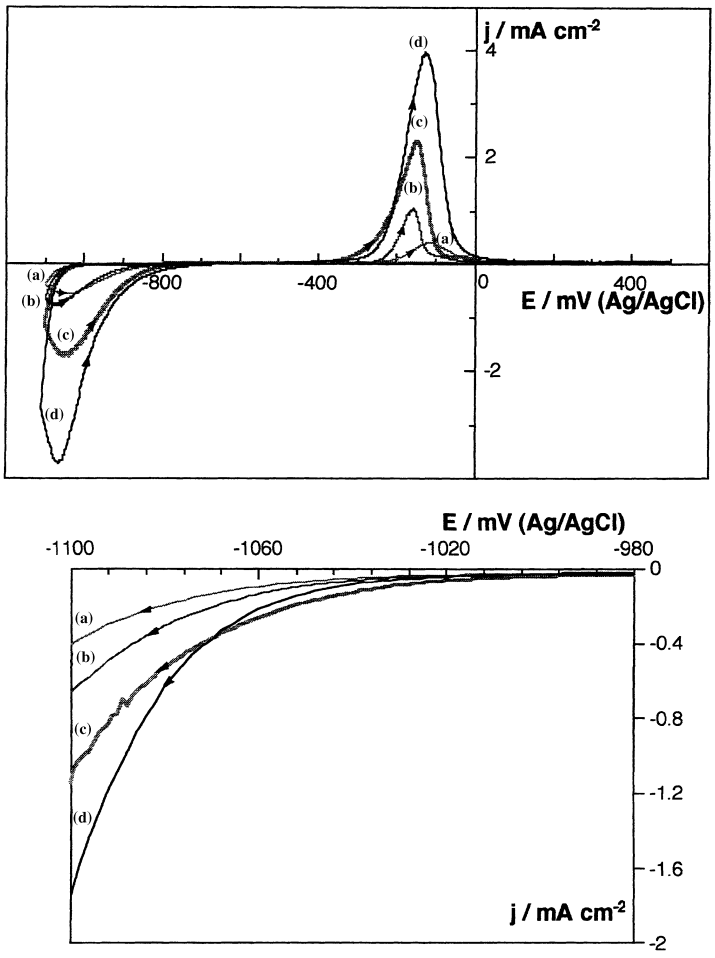

Fig. 2. Cyclic voltammograms at fixed cathodic limit: -1100 mV, $v = 50$ mV s^{-1}. General voltammograms and zoomed details. Solutions with 0.1 mol dm^{-3} $NiCl_2$ + x mol dm^{-3} $CoCl_2$. (a) $x = 0.002$, (b) $x = 0.007$, (c) $x = 0$, (d) $x = 0.013$.

favoured as the charge recorded increased (Fig. 2, curve (b)). However, even at these Co(II) concentrations, the total charge did not attain the value obtained from a cobalt-free solution (Fig. 2, curve (c)). It was necessary to add cobalt (II) up to 8×10^{-3} M to equal this charge.

With subsequent additions it was observed that upon increasing Co(II) concentration, the voltammetric current appeared at less negative potentials and the slope of the j/E voltammetric curve increased (Fig. 2, curve(d)), that is, the process was favoured. For this reason, while the voltammetric cathodic limit was maintained, the total charge increased with cobalt(II) concentration, to a greater extent than the corresponding increase in metallic ion concentration (Fig. 3).

3.2. *Galvanostatic experiments*

Additional chronopotentiometric experiments were performed using carbon electrodes modified by the presence of either nickel or cobalt freshly deposited. The modified electrodes were obtained by depositing the metal on vitreous carbon for 70 s at $-0.6\,\mathrm{mA\,cm^{-2}}$, which was sufficient time to ensure the total coverage of the electrode. Low current densities were chosen in order to minimize hydroxide formation. Galvanostatic curves were recorded for the deposition of cobalt on both cobalt and nickel freshly deposited. Then, the curves were also recorded for the deposition of nickel on both metals freshly deposited.

The deposition of each metal on fresh deposits of the same metal showed a predictable behaviour: no nucleation spike was detected and stationary current was attained a few seconds after the beginning of the deposition (Fig. 4, curves (a) and (c)).

When nickel was deposited on freshly deposited cobalt, a nucleation spike was observed, although, reasonably, the values obtained were less negative than on vitreous carbon (Fig. 4, curve (b)).

The results obtained for the deposition of cobalt on freshly deposited nickel were more interesting since at the first deposition times, the required current was attained at very low potentials (Fig. 4, curve (d)). For longer times, the potential evolved to the characteristic growth potential.

3.3. *Influence of deposition parameters*

A systematic study of the influence of deposition parameters such as deposition time, stirring of solution and applied potential was carried out, to assess the

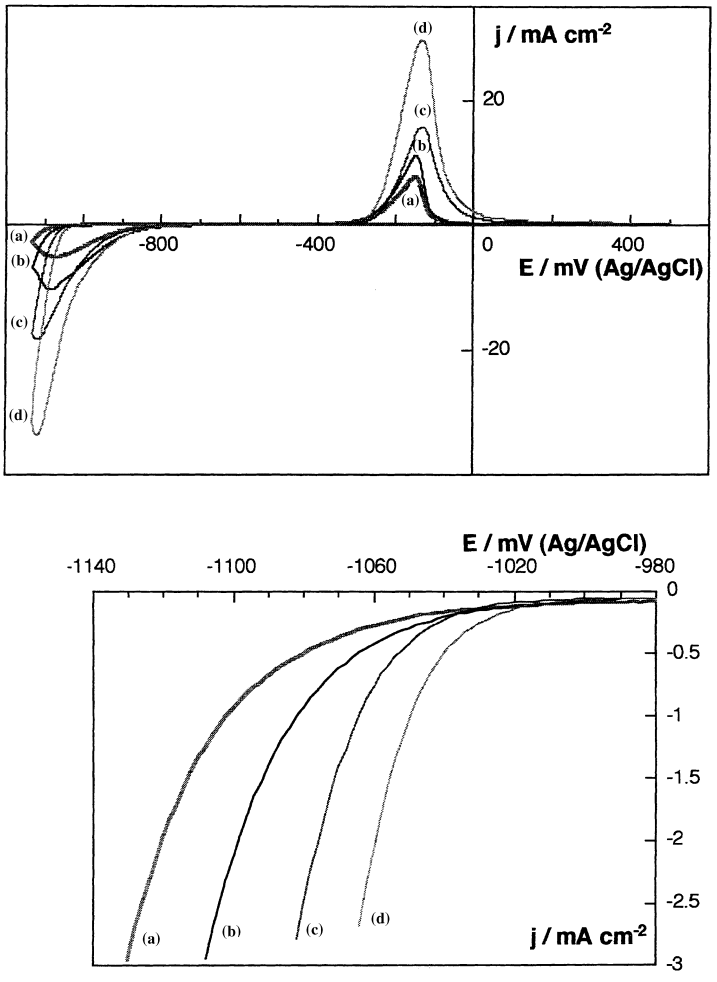

Fig. 3. Cyclic voltammograms at fixed cathodic limit: $-1130\,\mathrm{mV}$, $v = 50\,\mathrm{mV\,s^{-1}}$. General voltammograms and zoomed details of the beginning of the deposition zone. Solutions with $0.1\,\mathrm{mol\,dm^{-3}}$ $NiCl_2$ + $x\,\mathrm{mol\,dm^{-3}}$ $CoCl_2$ (a) $x = 0$, (b) $x = 0.012$, (c) $x = 0.054$, (d) $x = 0.097$.

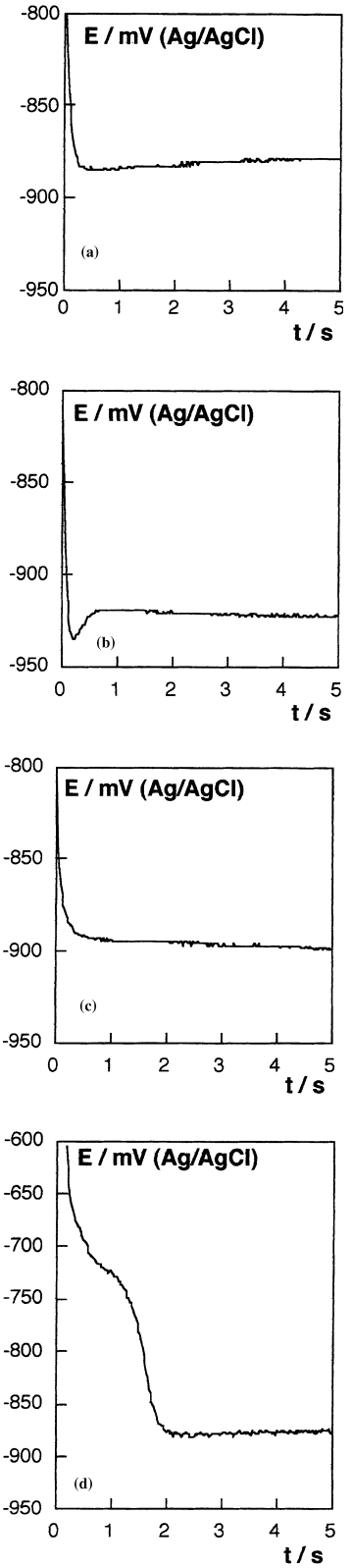

Fig. 4. Galvanostatic transients for metal deposition. Current density: $-0.6\,mA\,cm^{-2}$. (a) $0.1\,mol\,dm^{-3}$ $CoCl_2$ on C/freshly deposited Co, (b) $0.1\,mol\,dm^{-3}$ $NiCl_2$ on C/freshly deposited Co, (c) $0.1\,mol\,dm^{-3}$ $NiCl_2$ on C/freshly deposited Ni and (d) $0.1\,mol\,dm^{-3}$ $CoCl_2$ on C/freshly deposited Ni.

effect of these parameters both on the electrochemical response and on the morphology and composition of the deposits obtained. To this end, a fixed $0.1\,mol\,dm^{-3}$ $NiCl_2 + 0.012\,mol\,dm^{-3} CoCl_2$ solution was selected because this solution corresponded to a value at which

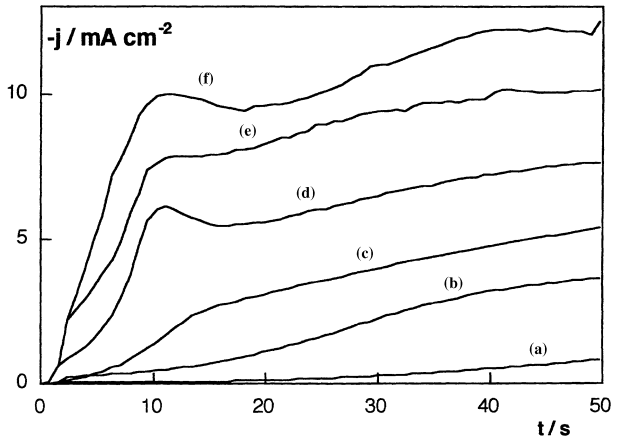

Fig. 5. *j–t* transients for $0.1\,mol\,dm^{-3}$ $NiCl_2$ + $0.012\,mol\,dm^{-3}$ $CoCl_2$ solution. (a) −925, (b) −950, (c) −975, (d) −1000, (e) −1025 and (f) −1050 mV.

the deposition process is favoured respect to the free cobalt solution and the posterior results confirmed that there is high cobalt ratio in the deposit. The potentiostatic technique was used to obtain the deposits.

Figure 5 shows the *j–t* transients obtained at different potentials in stationary conditions for the alloy deposition. At low overpotentials, the current increased smoothly; but upon increasing the potential, a slight slope change was observed as a peak developed, followed by a new increase in current, which then decreased with time. Moreover, the shape of the transients obtained for high potentials was disturbed by the simultaneous hydrogen evolution.

To analyse the influence of deposition time on the deposit composition, the deposits were obtained at low potentials. The composition of different deposits was analysed using X-ray microanalysis. In Table 1 the comparison of the results for deposits obtained at fixed potential, with and without stirring is shown. These data corroborated that anomalous codeposition also occurred in these conditions, and the proportion of cobalt in the deposits was greater than in the solution. When nickel(II) was the main component, in stationary conditions an increase in deposition time caused a clear decrease in cobalt content in the deposit. In contrast, when stirring was applied, no variation or very little variation of the deposit composition was observed over time.

On the other hand the influence of potential on deposit composition is shown in Fig. 6. Two parallel experiments were made using the same deposition

Table 1. Co/Ni ratio in the deposits formed as a function of time of deposition

Ni(II) 0.1 mol dm^{-3} + Co(II) 0.012 mol dm^{-3}

E/mV	*t*/s	*Co/Ni*	
		$\omega = 0$ rpm	$\omega = 1000$ rpm
−925	90	2.6	2.6
−925	300	1.2	2.5
−925	1200	0.8	2.3

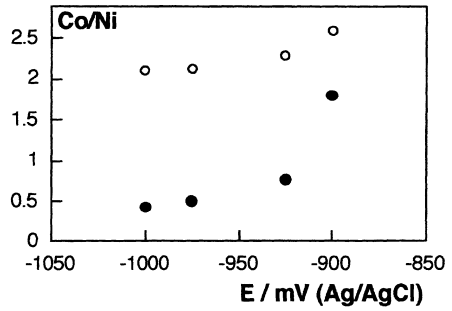

Fig. 6. Co/Ni ratio in the deposits obtained from a 0.1 mol dm^{-3} $NiCl_2$ + 0.012 mol dm^{-3} $CoCl_2$ solution, at different potentials. Key: (●) $\omega = 0$ rpm, (○) $\omega = 1000$ rpm. $Q = 100$ mC.

time. Whether using stationary conditions or stirring the solution, the X-ray microanalysis results indicated that, the Co/Ni ratio in the deposit always decreased when potential was increased.

Simultaneously, ALSV was chosen to test *in situ* the electrodeposits obtained potentiostatically both in stationary conditions and under agitation. At first, by comparing the *j–t* transients registered with and without stirring, no evident slope change was observed in stirred conditions (Fig. 7 upper diagram). Obviously, when deposition was carried out with stirring the total charge registered was greater. However, significant differences were observed between the anodic voltammograms recorded from these deposits, especially when they were obtained at longer deposition times or at high overpotentials. For a deposit obtained under stirring the stripping voltammogram showed only the peak corresponding to alloy oxidation, whereas when the deposition took place in stationary conditions additional peaks appeared at more positive potentials than that corresponding to the metallic alloy (Fig. 7 lower diagram).

Moreover, the SEM studies indicated that homogeneous compact deposits were found for longer deposition times. Deposits produced with stirring were more homogeneous and fine-grained than those produced in stationary conditions (Fig. 8). Their morphology was also different: under agitation, it was more edged.

3.4. *Influence of* [Co(II)]

Series of concentrations were made, maintaining Ni(II) concentration at 0.1 mol dm^{-3} and varying Co(II) concentration in the range 0–0.15 mol dm^{-3}. To attain a constant composition for all the deposition time, deposits were obtained using agitation. For each concentration analysed, the deposits were obtained at different applied potentials, maintaining the charge involved constant during the deposition. Parallel analysis of the composition and morphology of the deposits was made in all cases.

The deposits obtained at low potentials were always homogeneous but a gradual morphological modification was observed: they were more fine-grained when the proportion of Co(II) in solution was increased (Fig. 9). For the same applied potential the nucleation was favoured with Co(II) concentration as correspond to a gradual advance of the process. All deposits obtained were edged, as correspond to a cobalt-rich deposits (Fig. 10) [10].

The deposits obtained at more negative potentials from solutions with low Co(II) proportion were cracked (Fig. 11(a)), and had a similar morphology to the pure nickel deposits obtained at high overpotentials [11]. In these cases, the microanalysis indicated a high proportion of nickel in the deposits.

At these same potentials, upon increasing [Co(II)] in solution, the deposits were less cracked and more

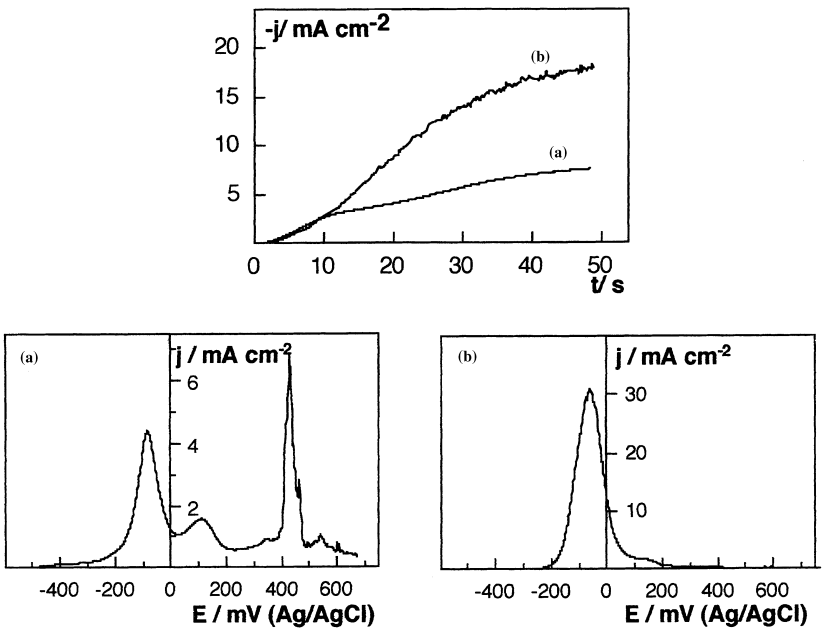

Fig. 7. (Upper) *j–t* transients for 0.1 mol dm^{-3} $NiCl_2$ + 0.012 mol dm^{-3} $CoCl_2$ solution. −990 mV. (a) $\omega = 0$ rpm, (b) $\omega = 1000$ rpm. (Lower) The corresponding stripping voltammograms of deposits. $v = 10$ mV s^{-1}.

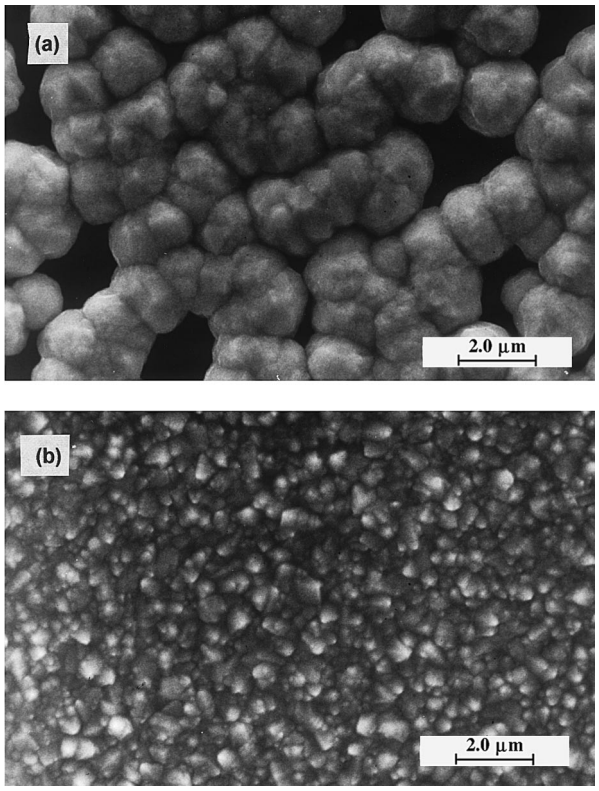

Fig. 8. SEM images of deposits obtained at −925 mV at $Q = 100$ mC, from a 0.1 mol dm^{-3} $NiCl_2$ + 0.012 mol dm^{-3} $CoCl_2$ solution (a) $\omega = 0$, (b) $\omega = 1000$ rpm.

uniform (Fig. 11(b)) with a gradual increase of cobalt content. The deposits obtained from the solution richest in Co(II) were homogeneous, compact and edged (Fig.11(c)).

When the cobalt(II) proportion was similar to the nickel(II) one, the deposits were very rich in cobalt (Table 2), although in stationary conditions the cobalt percentage also diminished with deposition time.

4. Discussion and conclusions

Cobalt–nickel alloys were electrodeposited in an acid bath containing different ratios of metallic cations. The chloride bath at pH 3 was found to be a suitable medium for cobalt–nickel deposition, because it permitted deposition of the alloy at relatively low cathodic potentials at low temperatures. Hydrogen evolution is minimized in these conditions.

Cobalt–nickel deposits with different proportions of the metals can be obtained using different deposition parameters, but preferential deposition of cobalt metal occurs and anomalous codeposition takes place. The control of these parameters permits the establishment of the deposition conditions that lead to the deposit appropriate to each application. For example, thin magnetic films require a high cobalt percentage in the deposits [2]. To this end, low cobalt (II) concentrations are sufficient to obtain high cobalt content in the film. Moreover, for a fixed solution composition, it is possible to vary the cobalt content using different deposition potentials: a decrease in the potential favours an increase in nickel

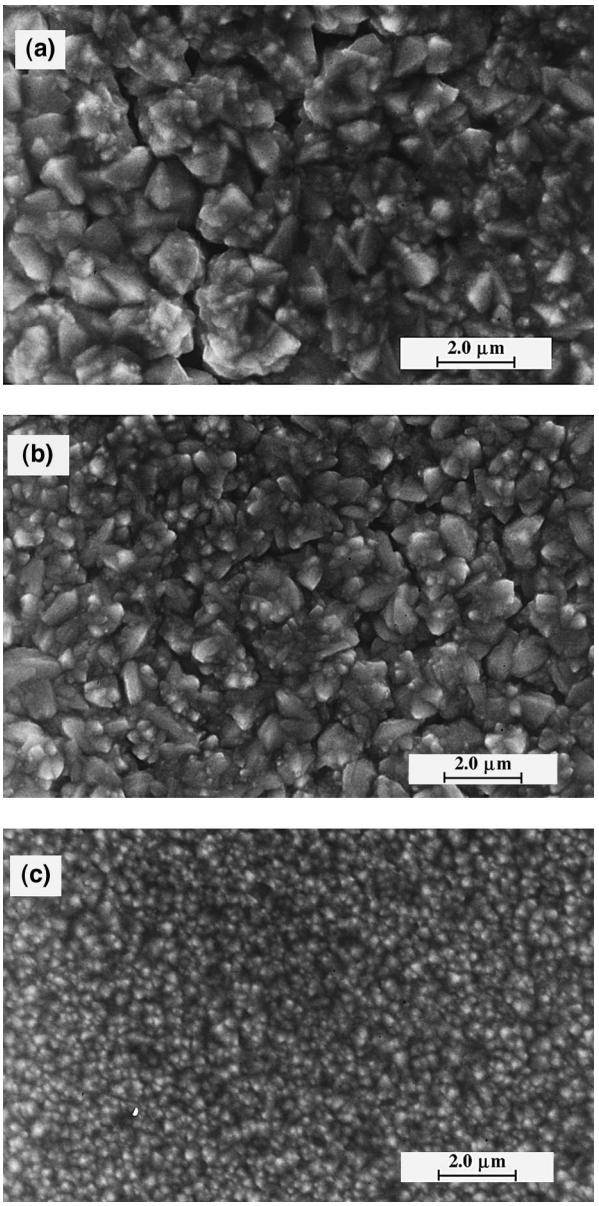

Fig. 9. SEM images of deposits obtained at −950 mV. $Q = 40$ mC. $\omega = 1000$ rpm. 0.1 mol dm^{-3} $NiCl_2$ + (a) 0.013, (b) 0.050, (c) 0.121 mol dm^{-3} $CoCl_2$.

percentage in the deposits. This is because the plating of Co–Ni alloys proceeds with simultaneous discharge of nickel(II) ions under activation control and cobalt(II) discharges under diffusion control. For this reason, a decrease in the applied potential diminishes

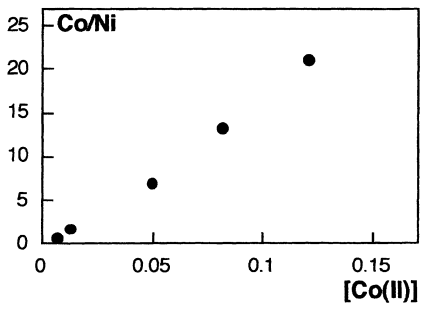

Fig. 10. Co/Ni ratio in the deposits obtained at −950 mV, $Q = 40$ mC. Solutions 0.1 mol dm^{-3} $NiCl_2$ + [Co(II)] mol dm^{-3}. $\omega = 1000$ rpm.

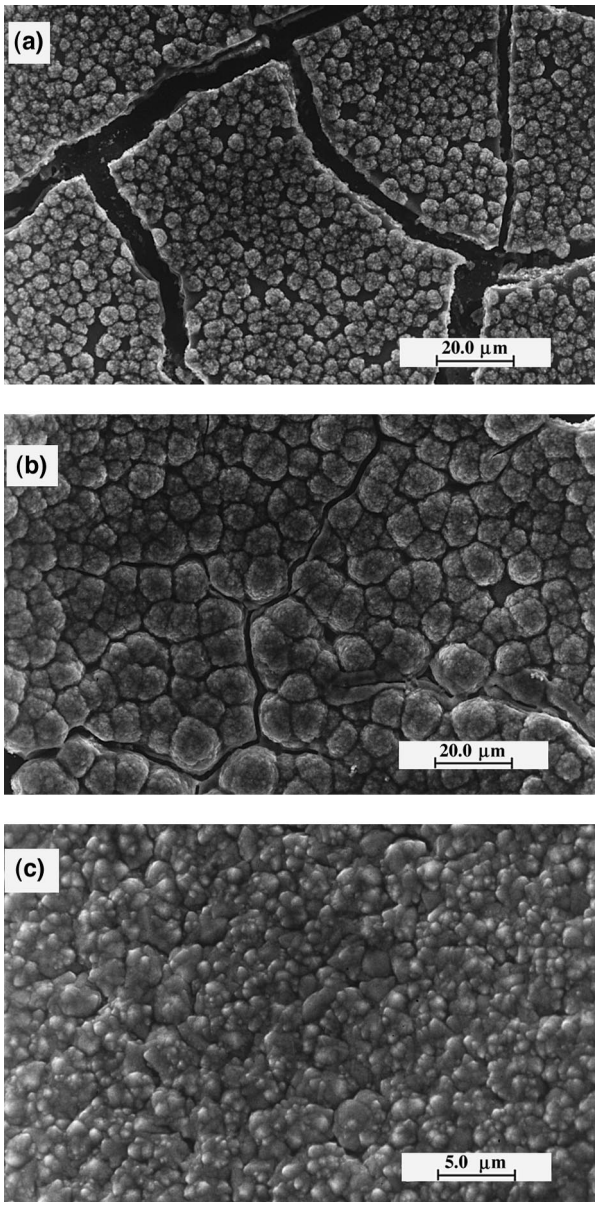

Fig. 11. SEM images of deposits obtained at −1050 mV. $Q = 40$ mC. $\omega = 1000$ rpm. 0.1 mol dm^{-3} $NiCl_2$ + (a) 0.007, (b) 0.013, (c) 0.121 mol dm^{-3} $CoCl_2$.

the great nickel polarization, which subsequently enhances the rate of deposition of nickel.

Deposit morphology varied with both bath composition and deposition potential. More homogeneous, fine-grained deposits can be obtained by increasing the cobalt(II)/nickel(II) ratio in solution, using low deposition potentials and stirring the solution.

Table 2. Co/Ni ratio in the deposits formed, at stationary conditions, as a function of time of deposition

Ni(II) 0.05 mol dm^{-3} + Co(II) 0.05 mol dm^{-3}
$E = -940$ mV

t/s	*Co/Ni*
22	10.0
60	5.5

Stirring the solution prevents the decrease in cobalt(II) (minority electroactive species in solution) in the environment of the electrode during the deposition. Stirring is also necessary to ensure that the alloy composition remains constant throughout the thickness of the deposit.

The electrochemical study of Co–Ni alloy deposition shows that only one oxidation peak is found for the deposits on vitreous carbon electrodes, both in voltammetric and in ALSV curves, as occurs for some solid solutions [12]. The oxidation peak appears at intermediate potential between the potentials of the oxidation peaks of pure cobalt and pure nickel, indicating that the structure of the deposit is similar to that of the pure metals. Then, these techniques do not enable the exact proportion of cobalt and nickel in the deposits to be defined. However, the ALSV technique is useful to define the range of potentials for which the deposits obtained are adequate, since it allows detection of secondary processes during the deposition: when hydroxides form, 'new' peaks appeared in ALSV curves at more positive potentials than that corresponding to the typical alloy oxidation. These new peaks are due to the presence of precipitated hydroxides, which hinder the oxidation of the alloy. The precipitation is a consequence of variation in local pH caused by simultaneous hydrogen evolution; this variation may be reflected in the slope change in the j–t transients recorded at stationary conditions and at high cathodic potentials. The formation of hydroxides inhibits the deposition process, and induces the formation of the cracked nonhomogenous deposits of the alloy observed at high cathodic potentials.

The stirring of the solution minimizes the inhibition process detected at high deposition rates and permits the use of a wider range of potentials for which deposits display a homogeneous and fine-grained morphology.

In the attempt to explain the cause of the anomalous codeposition of cobalt and nickel, the voltammetric technique has been revealed as a very useful tool.

The voltammetric results show that the beginning of nickel deposition occurs at more positive potentials than those corresponding to cobalt at similar concentration. Then, when both nickel and cobalt ions are present in the solution, the nickel is always deposited first.

When some nickel is deposited on the electrode, cobalt(II) species adsorb on the freshly electrodeposited nickel, hindering the normal nickel deposition, as can be observed for solutions with 0.1 M $NiCl_2$ and very low concentrations of cobalt(II). In these cases, the current due to cobalt deposition is very low and the overall result is an inhibition of nickel deposition.

When nickel(II) and cobalt(II) are present in solution, two parallel deposition processes take place: the nickel deposition, hindered by the presence of cobalt(II), and the deposition of cobalt. Upon increasing the Co(II) concentration, the voltammetric curve

gradually advances. Moreover, the charge recorded for a fixed cathodic limit increases in a greater proportion than that expected for the increase of the cobalt(II) concentration in solution.

These results show that, although the nickel deposition is initially inhibited by the presence of cobalt(II) in the solution, the alloy deposition process is favoured by an increase in the cobalt(II) concentration. A cobalt(II) species adsorbs on the freshly deposited nickel, which hinders subsequent nickel deposition, although it does not block it. Simultaneously, cobalt deposition is catalysed since it is enhanced on the nickel freshly deposited respect to the deposition on cobalt.

This proposal is supported by the results obtained from galvanostatic experiments of nickel and cobalt deposition on freshly electrodeposited metals. As expected, the deposition of each metal on itself is easy and the galvanostatic curves do not present the characteristic nucleation spike, and rapidly attain the characteristic growth potential. When nickel deposits on freshly deposited cobalt, a typical nucleation spike appears, revealing that an extra potential is necessary to begin the deposition. However, the cobalt deposition on freshly deposited nickel is easy and favoured respect to the cobalt on cobalt. This is probably due to a favoured electron transfer of cobalt(II) adsorbed on nickel or to the increase of some adsorbed species of cobalt that can be an intermediate in the mechanism of cobalt deposition, as occurs for nickel deposition.

Acknowledgements

The authors are indebted to the Serveis Cientifico-Tècnics of the Universitat de Barcelona for their support with SEM studies. We acknowledge financial assistance from the Comisión de Investigación Científica y Técnica (project MAT 94-1938). Thanks to Comissionat de Universitats de la Generalitat de Catalunya under Research Project SGR 344 (1995).

References

[1] S. N. Srimathi, S. M. Mayana and B. S. Sheshadri. *Surf. Technol.* **16** (1982) 277
[2] G. Bate, *in* 'Ferromagnetic Materials.' Vol. 2 (edited by E. P. Wohlfarth), North-Holland Publishing, (1980).
[3] J. P. Reekstini. *J. Appl. Phys.* **42** (1971) 1362
[4] C. Bajorek, S. Krongelb, L. T. Romankiw and D. A. Thompson, AIP Conference Proceedings, **24** (1974) 548.
[5] K. Ohashi, M. Ito and M. Watanabe, *in* 'Electrochemical Technology in Electronics', (edited by L. T. Romankiw and T. Osaka), The Electrochemical Society Softbound Proceedings Series, Pennington, NJ (1988), PV 88-23, p. 285.
[6] H. Barker (Ed), 'ASM Handbook', ASM International, Ohio (1992).
[7] A. Brenner, 'Electrodeposition of Alloys', Vol. 2, Academic Press, New York (1963).
[8] S. S. Abd El-Rehim, A. M. Abd El-Halim and M. M. Osman. *J. Appl. Electrochem.* **15** (1985) 107.
[9] Ch. Fan, D. L. Piron, M. Meilleur and L. P. Marin, *Can. J. Chem. Eng.* **71** (1993) 570.
[10] M. L. Alcalá, E. Gómez and E. Vallés, *J. Electroanal. Chem.* **370** (1994) 73.
[11] E. Gómez, C. Muller, R. Pollina, M. Sarret and E. Vallés. *ibid.* **333** (1992) 47.
[12] V. D. Jovic, R. M. Zejnilovic, A. R. Despic and J. S. Stevanovic. *J. Appl. Electrochem.* **18** (1988) 511.